Knockout silkworms reveal a dispensable role for juvenile hormones in holometabolous life cycle

Takaaki Daimon[a,1], Miwa Uchibori[a], Hajime Nakao[a], Hideki Sezutsu[b], and Tetsuro Shinoda[a]

[a]Division of Insect Sciences, National Institute of Agrobiological Sciences, Owashi 1-2, Tsukuba City, Ibaraki, 305-8634, Japan; and [b]Genetically Modified Organism Research Center, National Institute of Agrobiological Sciences, Owashi 1-2, Tsukuba City, Ibaraki, 305-8634, Japan

Insect juvenile hormones (JHs) prevent precocious metamorphosis and allow larvae to undergo multiple rounds of status quo molts. However, the roles of JHs during the embryonic and very early larval stages have not been fully understood. We generated and characterized knockout silkworms (Bombyx mori) with null mutations in JH biosynthesis or JH receptor genes using genome-editing tools. We found that embryonic growth and morphogenesis are largely independent of JHs in Bombyx and that, even in the absence of JHs or JH signaling, pupal characters are not formed in first- or second-instar larvae, and precocious metamorphosis is induced after the second instar at the earliest. We also show by mosaic analysis that a pupal specifier gene broad, which is dramatically up-regulated in the late stage of the last larval instar, is essential for pupal commitment in the epidermis. Importantly, the mRNA expression level of broad, which is thought to be repressed by JHs, remained at very low basal levels during the early larval instars of JH-deficient or JH signaling-deficient knockouts. Therefore, our study suggests that the long-accepted paradigm that JHs maintain the juvenile status throughout larval life should be revised because the larval status can be maintained by a JH-independent mechanism in very early larval instars. We propose that the lack of competence for metamorphosis during the early larval stages may result from the absence of an unidentified broad-inducing factor, i.e., a competence factor.

juvenile hormone | metamorphosis | ecdysone | TALEN | Bombyx

Insect molting and metamorphosis are intricately governed by two hormones, ecdysteroids and juvenile hormones (JHs) (1–3). Ecdysteroids, which are produced in the prothoracic gland, trigger each larval–larval and metamorphic molt, whereas JHs, which are produced in the corpora allata (CA), prevent precocious metamorphosis and allow the larva to undergo multiple rounds of molting until it reaches the appropriate size for metamorphosis (1–5). It is widely considered that this "status quo" action of JH is required to maintain the larval status throughout the larval stage. Interestingly, however, several attempts to deplete JHs using classic and modern techniques have failed to induce precocious metamorphosis during the very early larval instars (6–12).

In the classic experiments by Bounhiol (11) and Fukuda (12), allatectomy (surgical removal of the CA) or neck ligation (separation of the head containing the CA from the posterior part of the body) in lepidopteran larvae induced precocious metamorphosis; however, the earliest instar that exhibited the signs of metamorphosis was the third. Chemical allatectomy, i.e., the application of compounds that inhibit the biosynthesis of JHs, also can induce precocious metamorphosis, but larvae that receive chemical allatectomy during the embryonic or first larval instar stages do not undergo metamorphosis until after the second instar (in the locust) (13) or the third instar (in the silkworm Bombyx mori) (14). Recent genetic studies also have shown that deprivation of JHs cannot induce precocious metamorphosis during the early larval instars. For example, overexpression of a JH-degrading enzyme JH esterase (JHE) in transgenic Bombyx

resulted in precocious metamorphosis after three instars (8). In addition, the dimolting (mod) mutant larvae of Bombyx with a null mutation in a JH biosynthetic enzyme, JH epoxidase CYP15C1, metamorphosed into miniature pupae after the third or fourth instar (7). Similarly, RNAi of a JH receptor Methoprene tolerant (Met) or Krüppel-homolog 1 (Kr-h1), a repressor of pupal metamorphosis, in the early instars of a hemimetabolous Pyrrhocoris bug did not cause precocious metamorphosis until after the third instar (6). In addition, in the fruit fly Drosophila melanogaster, deprivation of the CA or double mutation of two paralogous JH receptor genes, Met and germ cell expressed (gce), did not reduce the number of molts (9, 10). These results consistently suggest that the development of early larval instars is largely independent of JHs and that the antimetamorphic action of JHs is required only in the later larval stages to prolong these larval stages until the larvae attain an appropriate threshold size for metamorphosis.

This hypothesis is not fully supported, however, because there were some weaknesses or problems in the aforementioned experiments; for example, (i) it is still possible that residual JHs suppress precocious metamorphosis in larvae that have been subjected to surgical or chemical allatectomy; (ii) degradation of JHs may not be complete in JHE-overexpressing Bombyx larvae; (iii) gene silencing using RNAi is transient and incomplete; (iv) the antimetamorphic action of JHs in Drosophila, in which the number of larval instars appears to be firmly fixed at three, is not as obvious as that in most other insects; and (v) mod mutant larvae of Bombyx actually lack JHs in the hemolymph, but their CA may produce a JH precursor, methyl farnesoate (MF) (7), which has a very weak JH activity [i.e., 1,000-fold lower activity compared with the authentic epoxidized JH I in the induction of

Significance

The juvenile–adult transition is a key developmental process in organisms. A long-held paradigm in insect endocrinology is that juvenile hormones (JHs) prevent metamorphosis until larvae attain an appropriate size for the juvenile–adult transition. However, little is known about the roles for JHs during embryonic and very early larval stages. We established knockouts of the silkworm, a classic model insect, and show that embryogenesis and maintenance of juvenile status during the early larval stages are largely independent of JHs or the JH-signaling pathway. Our results also suggest that an unidentified factor or signal is required to acquire the competence for metamorphosis. The presence of this factor has long been overlooked because JHs may conceal its action.

the Kr-h1 gene in cultured cells (15)], and thus MF may partially rescue the absence of JHs in *mod* mutant larvae.

To avoid these problems and to obtain definitive evidence to reveal the roles of JHs during the early larval instars, we performed knockout experiments targeted at genes involved in JH biosynthesis and JH reception in *Bombyx*, in which a highly efficient system for targeted mutagenesis mediated by transcription activator-like effector nucleases (TALENs) has been established (16, 17). We generated a knockout mutant of *JH acid methyltransferase* (*JHAMT*) (18), which catalyzes the last step of JH biosynthesis in lepidopteran insects, as well as the two JH receptor genes in *Bombyx*, *Met1*, and *Met2* (15). Our results demonstrated that JHs or JH signaling does not play important roles in embryogenesis in *Bombyx*, and even in the absence of JHs or JH signaling pupal characters (i.e., pupal cuticles, degeneration of larval abdominal legs, and metamorphic growth of imaginal primordia) are not observed in the first- or second-instar larvae; these results strongly support the hypothesis that development in early larval instars is independent of JHs. We also showed, based on a TALEN-mediated somatic mosaic analysis, that a pupal-specifier gene *broad*, which is dramatically up-regulated in the late stage of the last larval instar (19–22), is essential for pupal commitment in the epidermis of *Bombyx*. Importantly, the mRNA expression level of *broad*, which is considered to be repressed by JHs until the late stage of the last larval instar (19–22), remained at very low basal levels during the first and second larval instars of JH-deficient or JH signaling-deficient knockouts. Therefore, the results of our study suggest that the lack of competence for metamorphosis during the early larval stages may be attributable to the absence in the very early stages of an unidentified *broad*-inducing factor, i.e., a competence factor, that is required for the metamorphic induction of *broad*.

Results

TALEN-Mediated Knockout of *JHAMT*, *Met1*, and *Met2* Genes.
In the last step of the JH biosynthetic pathway in *Bombyx* (Fig. 1A), a JH precursor, farnesoic acid, is epoxidized to JH acid by CYP15C1 and then is methylated to the final product JH by JHAMT (5, 7). It should be noted that *Bombyx* has two paralogous JH receptor genes, *Met1* and *Met2* (15), which may have been duplicated independently after the divergence of the order Lepidoptera (moths and butterflies) and Diptera (flies and mosquitoes) (23–25). Therefore, by using TALENs, we used two approaches to generate JH-deficient or JH signaling-deficient mutants (Fig. 1B): first, we knocked out the *JHAMT* gene, and second, we knocked out the *Met1* and *Met2* genes. We injected TALEN mRNAs, which specifically target the first or second exons of these genes, into early embryos of *Bombyx* and established single-knockout lines for each gene. Deletions in these lines (88 bp for *JHAMT*, 44 bp for *Met2*, and 67 bp for *Met1*) introduce premature stop codons into domains that are essential for their functions (i.e., the methyltransferase domain in *JHAMT* and a DNA-binding basic helix–loop–helix domain in *Met1* and *Met2*). Therefore these knockout alleles should be null alleles (Fig. 1B and Fig. S1). Next, double-mutant lines for *JHAMT mod* and *Met2 Met1* were established after crossing *JHAMT* heterozygous mutants with *mod* mutants (7, 26) and *Met2* homozygous mutants with *Met1* heterozygous mutants. Because homozygous mutations of *JHAMT* and *Met1* are lethal (as described below), the *JHAMT*- and *Met1*-mutant alleles were maintained as heterozygous stocks (*Materials and Methods*).

Effects of JH Deprivation or JH Signaling Deprivation During the Embryonic Stages.
It has been suggested that JHs are not important for embryogenesis in holometabolous insects because the application of JHs to the fertilized eggs of wild silkmoths cannot block embryonic development before the completion of a rec-
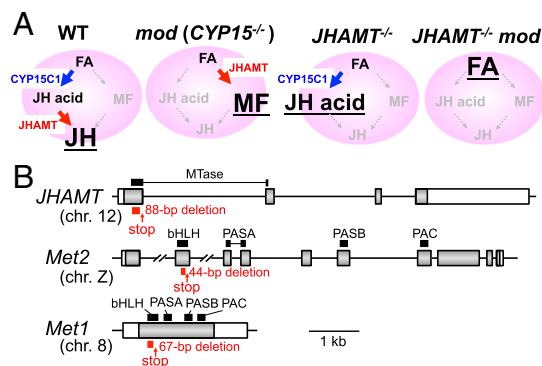

Fig. 1. TALEN-mediated gene disruption. (A) JH biosynthetic pathways in wild-type and mutant *Bombyx*. In the CA of wild-type *Bombyx*, farnesoic acid (FA) is epoxidized to JH acid by CYP15C1 and JH acid then is methylated to the JH by JHAMT (5). In the CA of *mod* and *JHAMT* mutants and *JHAMT mod* double mutants the presumed products are MF, JH acid, and FA, respectively (underlined). Note that the major JHs and their precursors (not illustrated in the figure) are ethyl-branched in lepidopteran insects (5, 7). (B) Schematic representations of mutant alleles used in this study. For *JHAMT*, *Met2*, and *Met1* mutants, we fixed 88-, 44-, and 67-bp deletion alleles, respectively, and used them in further experiments. Gray and white bars indicate the coding regions and UTRs, respectively. Horizontal lines flanked by exons indicate introns. Red lines below the exons indicate deleted regions, and red arrows indicate the positions of premature stop codons caused by deletions. Chromosomal localizations of each gene are shown in parentheses. The nucleotide sequence of each allele is shown in Fig. S1. bHLH, basic helix–loop–helix domain; MTase, methyltransferase domain; PAC, PAC domain (24); PASA, Per-ARNT-Sim A domain; PASB, Per-ARNT-Sim B domain. (Scale bar: 1 kb.)

ognizable first instar, although treatment of early embryos with JH results in abnormal blastokinesis (27). We observed the same phenomenon in JH-treated *Bombyx* embryos (Fig. S2A). However, the effects of JH deprivation during the embryonic stages have not been clarified in holometabolous insects because surgical allatectomy is virtually impossible in embryos and allatocidal chemicals that are active in holometabolous insects have not yet been identified. Therefore, we first examined the embryo phenotypes of JH-deficient or JH signaling-deficient mutants. We found that the hatchability of embryos was reduced (Fig. 2A) and the day of hatching was delayed by a few days in homozygous mutants of *JHAMT*, *JHAMT mod*, *Met1*, and *Met2 Met1* as compared with a control strain (Fig. 2B). In these mutant embryos, pigmentation of the trachea, which occurred on day 7 in the control, was delayed for ~1 d. These results indicate that deprivation of JH or JH signaling causes high or partial lethality in embryos and delays embryonic development. Therefore, we next examined the expression profiles of the genes involved in JH biosynthesis and JH signaling during the embryonic stages (Fig. 2C). In the tobacco hornworm, *Manduca sexta*, it has been suggested that JH titers in embryos peak at about 50% of embryonic development and then decrease gradually (28, 29). Similarly, in *Bombyx*, we found that the expression of *JHAMT* increased sharply from 108 h after oviposition (AO) and remained high at 134 and 168 h AO before decreasing gradually. It was notable the timing of the increase in the two isoforms of Kr-h1 mRNA (Kr-h1α and Kr-h1β) (15) was the same as that of *JHAMT*, thus suggesting that JHs are synthesized de novo from this time. Large amounts of *Met1* and *Met2* mRNA appeared to be maternally deposited in embryos, but they decreased gradually to basal levels by 84 h AO and then increased from 96 h AO and peaked at 108 h AO, the time when the expression levels of *JHAMT* and Kr-h1 mRNA started to increase. Whole-mount in situ hybridization showed that the *JHAMT* mRNAs localized specifically to the CA (Fig. 2D), thereby demonstrating that JHs are produced in the CA during the embryonic (Fig. 2D) and
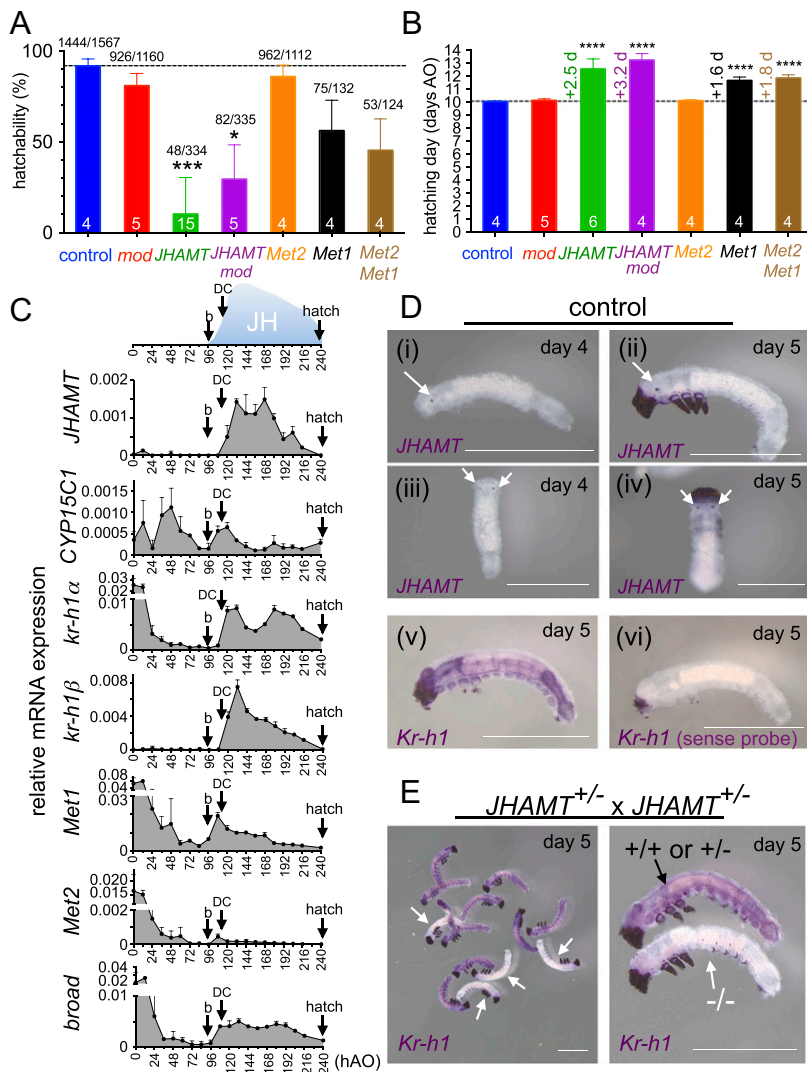
Fig. 2. Effects of knockouts on embryogenesis. (*A* and *B*) Hatchability (*A*) and day of hatching (*B*) by mutant strains. Hatched larvae or unhatched embryos (stage ≥25) (67) were counted, and their individual genotypes were determined by PCR if necessary. Mutated lines are shown below the bars. Bars indicate mean + SD for hatchability (*A*) or the hatching day AO (*B*) for each genotype (*n* = 4–15 batches). The numbers above bars indicate the number of hatched/total embryos, and the numbers within bars indicate the number of batches used in the analysis. Asterisks indicate significant differences compared with the control. *$P < 0.05$, ***$P < 0.001$, ****$P < 0.0001$, Dunn's nonparametric multiple comparisons test. (*C*) qRT-PCR of genes in the control strain. Data represent the mean + SD expression level of each gene (*n* = 4 biological replicates). The numbers below the *x* axis indicate hours AO. The presumed JH titer shown at the top is inferred from that in *Manduca* (28). Timings of the onset of blastokinesis (b) and completion of dorsal closure (DC) are based on Takami and Kitazawa (67). (*D*) Whole-mount in situ hybridization of *JHAMT* and *Kr-h1* in the control strain. Arrows indicate the CA-specific signals of *JHAMT*. Signals in the head and thoracic legs are caused by nonspecific staining. Stages (days AO) of samples are shown at the top right of each panel. (*i, ii, v,* and *vi*) Lateral view. (*iii* and *vi*) Dorsal view. (Scale bars: 1 mm.) (*E*) Whole-mount in situ hybridization of *Kr-h1* in *JHAMT*-knockout embryos. Embryos obtained from the sibling cross of *JHAMT*⁺/⁻ were subjected to analysis. About one-fourth of the embryos were not stained, as indicated by the white arrows. These unstained embryos were probably *JHAMT* homozygous mutants, as supported by the results of qRT-PCR (Fig. S6). (Scale bars: 1 mm.)

larval stages (7, 18). To determine the effects of JH deprivation on the expression of *Kr-h1*, we examined *Kr-h1* expression in the *JHAMT* mutants, which exhibited the most severe defects in hatchability (Fig. 2*A*). When embryos from a sibling cross of *JHAMT*⁺/⁻ adults were examined on day 5, at the peak of the *Kr-h1* mRNA levels in the control (Fig. 2*C*), about one-fourth of the embryos, which probably were *JHAMT* homozygous mutants (assuming a 1:2:1 segregation ratio via Mendelian inheritance), did not exhibit *Kr-h1* mRNA signals (Fig. 2*E*). This finding suggests that, as in the larval stages, JHs induce the expression of *Kr-h1* in the embryonic stages. Notably, these unstained (presumable *JHAMT*⁻/⁻) embryos were similar in size to the stained (*JHAMT*⁺/⁺ or *JHAMT*⁺/⁻) embryos.

Development of JH-Deficient Mutants. To test whether the reduced hatchability in *JHAMT* mutant embryos resulted from the loss of JHs, we performed rescue experiments by topically applying JHs to embryos (Fig. 3 *A* and *B*). First, we applied selected doses of JH III to embryos on day 4, 1 d before the presumed peak in the JH titers (Fig. 2*C*). As shown in Fig. 3*A*, the unhatched phenotype of *JHAMT*⁻/⁻ embryos was rescued by the application of JH III in a dose-dependent manner. The most effective dose of JH III was 0.1 µg (~90% of treated embryos hatched), and reducing or increasing this dose lowered the rate of hatching, suggesting that the presence of an appropriate amount of JHs is important

during embryogenesis. The application of a JH analog, methoprene, also rescued the unhatched phenotype of *JHAMT*⁻/⁻, but the most efficient dose was <0.001 µg (Fig. 3*A*). This result may appear puzzling, because methoprene generally has a much weaker JH activity than JH III [i.e., ~500-fold less activity than JH III in cultured cells (15)]; however, we believe this result probably was caused by differences in the biodegradability and/or permeability of JH III and methoprene. Treatment with MF, which has very weak JH activity [i.e., comparable with that of methoprene (15)], also rescued the phenotype, but its efficiency was much lower than that of JH III or methoprene. Next, we examined the temporal effect of JH III treatment and identified clear time-dependent effects (Fig. 3*B*). When JH III (0.1 µg, which had the highest rescue activity on day 4; Fig. 3*A*) was applied on day 4 or day 5, >90% of the *JHAMT*⁻/⁻ embryos were rescued, but application after day 7 appeared to be too late. These results suggest that JHs should be present in the appropriate amounts and at the appropriate times during embryogenesis. Surprisingly, we found that embryogenesis appeared to be completed in the "unhatched" *JHAMT*⁻/⁻ embryos, and they were alive within their eggshells. When we removed their eggshells with a knife (dechorionation), the dechorionated embryos (or now larvae) began to exhibit locomotory behaviors (Fig. 3*C* and Movie S1), and they fed and grew (Fig. 3*D*). This finding indicates that JH deprivation during the embryonic stages has
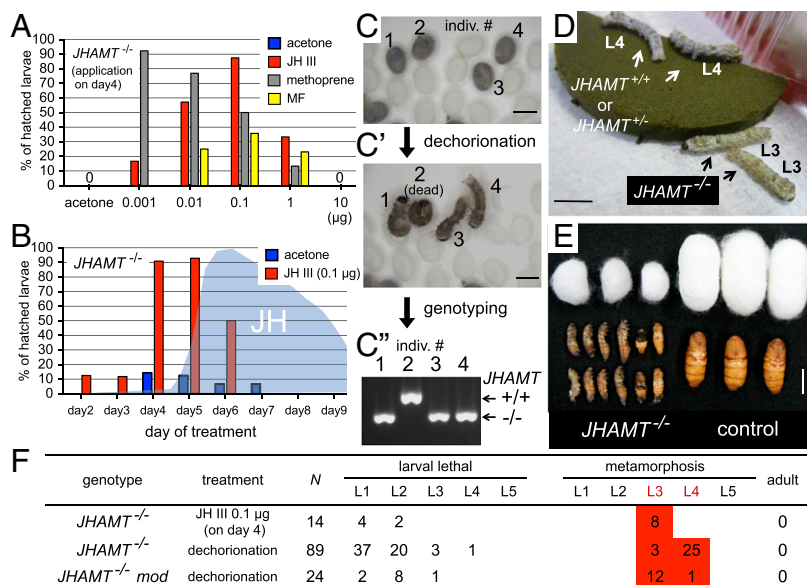
Fig. 3. Phenotypes of JH-deficient *Bombyx*. (*A*) Rescue experiments of *JHAMT*$^{-/-}$ embryos. Bars indicate the hatchability of *JHAMT*$^{-/-}$ embryos treated with selected amounts (0.001–10 µg) of JH III, methoprene, and MF on day 4 AO. Acetone was used as a solvent control. n = 7–16 individuals for each bar. (*B*) Time-dependent effects of JH III application. JH III (0.1 µg) was applied to *JHAMT*$^{-/-}$ embryos at selected time points, and their hatchability was recorded. n = 7–17 individuals for each bar. (*C*) Dechorionation of unhatched eggs from the sibling cross of *JHAMT*$^{+/-}$ moths. The image shows unhatched eggs on day 12 AO. After dechorionation, *JHAMT*$^{-/-}$ larvae (individuals #1, 3, and 4) commenced locomotory behaviors, but a *JHAMT*$^{+/+}$ larva (individual #2) was dead. Genotypes of the larvae shown in *C'* were determined by genomic PCR (*C''*). (Scale bars: 1 mm.) (*D*) Development of *JHAMT*$^{-/-}$ larvae treated with JH III (0.1 µg) on day 4 AO. *JHAMT*$^{-/-}$ larvae started wandering and spinning from L3, whereas the *JHAMT*$^{+/+}$ and *JHAMT*$^{+/-}$ larvae reached L4. (Scale bar: 1 cm.) (*E*) Dechorionated *JHAMT*$^{-/-}$ larvae (L4) became small larval and pupal intermediates. (Scale bar: 1 cm.) (*F*) Development of JH-deficient mutants, which underwent precocious metamorphosis after L3 at the earliest. No larvae reached L5.

genotype	treatment	N	larval lethal					metamorphosis					adult
			L1	L2	L3	L4	L5	L1	L2	L3	L4	L5	
JHAMT$^{-/-}$	JH III 0.1 µg (on day 4)	14	4	2						8			0
JHAMT$^{-/-}$	dechorionation	89	37	20	3	1				3	25		0
JHAMT$^{-/-}$ *mod*	dechorionation	24	2	8	1					12	1		0

only a minor effect and that embryonic growth and morphogenesis can proceed normally even without JHs. Indeed, dechorionated neonate larvae did not possess any specific external phenotypes when examined by scanning electron microscopy (SEM) (Fig. S3). It is unclear why JH deprivation leads to a hatching deficiency because the hormones or neurons responsible for hatching behaviors have not been clarified (30, 31). It is possible that JHs play roles in some parts of embryonic neurogenesis that are involved in hatching behavior. To elucidate the development of JH-deficient mutants, we reared *JHAMT*$^{-/-}$ larvae rescued by JH III application or dechorionation and found that about half of the hatched *JHAMT*$^{-/-}$ larvae grew well (Fig. 3 *D* and *E*) and eventually underwent precocious metamorphosis after the third larval instar (L3) at the earliest (Fig. 3*F* and Fig. S2*B*). Similarly, when unhatched *JHAMT mod* double-mutant embryos were dechorionated, about half of them grew and metamorphosed after L3 (Fig. 3*F*). Importantly, precocious metamorphosis was not observed at L1 or L2, and the larvae that died during L1 or L2 did not exhibit any specific external phenotypes. These results strongly suggest that larval status is maintained independently of JHs in L1 and L2.

Development of JH Signaling-Deficient Mutants. Next, we performed phenotypic analyses of *Met* mutants. *Met1* mutant larvae exhibited retarded growth (Fig. 4*A*), and their development was arrested predominantly during molting from L2 to L3. Most of them failed to shed their old L2 cuticles completely or partially (Fig. 4*B*), and all died without feeding. When the L2 cuticles of the arrested larvae were removed with forceps, the L3 *Met1*$^{-/-}$ larvae had the overall appearance of larvae (Fig. 4*C*). Interestingly, we found that small patches of pupal cuticle, which were not present in the L1 or L2 cuticle, had formed in the L3 cuticles (Fig. S4). The formation of these pupal patches was observed only in specific regions around the "bulge" (32) of the second and the third thoracic segments (T2 and T3) and the

dorsolateral side of the first abdominal segment (A1) (Fig. 4 *C* and *D*). In contrast, *Met2* mutants were viable and fertile, and they did not exhibit any apparent phenotypes. We also analyzed *Met2 Met1* double mutants and found that they phenocopied the *Met1* mutants (Fig. 4 *E* and *F*). These results suggest that *Met1* is the predominant JH receptor and that *Met2* plays a very minor role, if any, during the larval stages in *Bombyx*.

Mosaic Analysis of *Met1*. We also performed a mosaic analysis of *Met1* using the hereditary mosaic strain (*mo*) of *Bombyx* (Fig. 5). In this mosaic strain, the polar body nuclei do not degenerate in some eggs of *mo/mo* females, and the two nuclei from the egg and polar body are fertilized independently by sperm in a single egg, thereby yielding a single mosaic animal, not a twin (33–35). In severe cases, mosaic animals become half-and-half mosaics. In the mosaic analysis of *Met1*, we introduced the *Met1*-mutant allele into the *mo* strain and eventually established a *Met1* mosaic strain (*Materials and Methods*). In the progeny of this strain, *Met1* mosaic animals were segregated at a low frequency (<10%). Among 191 mosaic eggs that exhibited mosaic pigmentation patterns in amnioserosa, which is caused by another marker gene, *w-2*, 21 were *Met1* mosaic animals, according to their larval–pupal mosaic phenotypes. Importantly, 81% (17 of 21) of the *Met1* mosaic L3 larvae reached L4, allowing us to investigate the phenotypes of *Met1* mosaics at L4, i.e., one instar later than the *Met1* knockouts, which arrested during their L2–L3 molts (Fig. 4). As expected, some animals eventually became severe larval–pupal mosaics with pupal cuticles that covered about half of the body (individuals #96, 152, and 174 in Fig. 5*A*), thereby providing strong evidence that *Met1* is the cell-autonomous JH receptor. To determine when the pupal characteristics are first formed during development, we carefully checked for the presence of pupal features in L1–L3 larvae. We found that the earliest formation of pupal features was represented by patches of pupal cuticles (Fig. 5*B*), which were induced during the molt
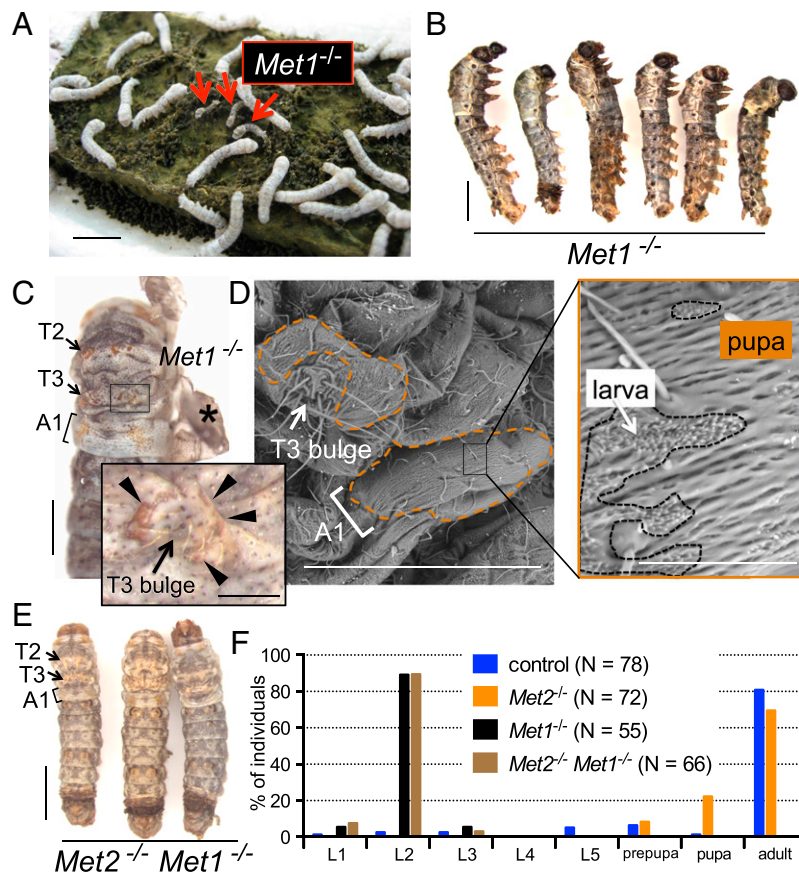
Fig. 4. Phenotypes of JH receptor mutants. (*A*) Image of L2 larvae obtained from the sibling cross of *Met1*^{+/−} adults. *Met1*-mutant larvae exhibited retarded growth (red arrows). (Scale bar: 1 cm.) (*B*) Most of the *Met1*-mutant larvae were developmentally arrested when molting from L2 to L3. (Scale bar: 2 mm.) (*C*) Formation of patched pupal cuticles in L3 *Met1* mutants. The old L2 cuticles of arrested *Met1* larvae were removed with forceps (asterisk). Pupal patches were found around the T2 and T3 bulges (32) and the dorsolateral region of A1. (Scale bar: 1 mm.) (*Inset*) Magnified view of the area around the T3 bulge with pupal patches (arrowheads) (Scale bar: 0.2 mm.) (*D*) SEM analysis of patches of pupal cuticles of L3 *Met1* larvae. Cuticles with pupal characteristics are indicated by dotted lines. A magnified view is shown on the right. (Scale bars: 500 μm, *Left* and 50 μm, *Right*.) (*E*) Image of *Met2 Met1* double mutants, which were developmentally arrested during the molt from L2 to L3. The positions of the pupal patches were very similar to those in *Met1* mutants. (Scale bar: 2 mm.) (*F*) Lethal stages in the control, *Met2*, *Met1*, and *Met2 Met1* mutants.

from L2 to L3 (individual #152 in Fig. 5*A*). This observation was very similar to our observation in *Met1* mutants in terms of timing and the region where the patches formed (Fig. 3*C*). However, the formation of the pupal patches in *Met1* mosaics was limited to the side on which drastic pupal metamorphosis was induced in the next molt (from L3 to L4). In *Met1* mosaics, the metamorphic growth of imaginal discs and primordia (i.e., wing discs, antennae, eyes, and legs), as well as the degeneration of larval abdominal legs, was induced after molting from L3 to L4 (Fig. 5 *C* and *D*) and not at molting from L2 to L3. In lepidopteran and coleopteran insects, the epidermal cells sequentially produce larval, pupal, and adult cuticles through development, but in higher Diptera such as *Drosophila*, the adult epidermis is derived from imaginal discs or histoblast cells (36). Therefore, our mosaic analysis showed that, except for very limited regions of the epidermal cells, the metamorphic molt and growth of imaginal discs was not induced in *Met1* mutant cells until molting from L3 to L4. This analysis provides evidence that larval status is maintained independently of JH signaling during L1 and L2. As proposed by Smykal et al. (6), our results may suggest that the competence for metamorphosis is acquired gradually during larval development, given that L3 tissues were much more sensitive than L2 tissues to the absence of JH signaling (Fig. S5).

Gene-Expression Analysis. Next, we investigated the expression of *Kr-h1* mRNA in the mutants generated in this study during their embryonic (Fig. S6) and larval stages (Fig. 6). As expected, the expression levels of *Kr-h1* mRNAs were reduced dramatically in both JH biosynthesis and JH receptor mutants during the embryonic (Fig. S6 *A* and *B*) and larval stages (Fig. 6*B*). Notably, the expression levels in *Met2* mutants were comparable with those in the control strain, supporting the notion that *Met2* plays almost no role in JH signaling during these stages. To determine whether the reduced expression levels were caused by the loss of JH biosynthesis or JH signaling, we tested the effect of methoprene treatment on the expression of *Kr-h1* mRNA (Fig. 6*C* and Fig. S6*C*). We found that *Kr-h1* expression was strongly induced by methoprene in JH biosynthesis mutants but not in *Met1* mutants or *Met2 Met1* double mutants, indicating that the knockouts generated in this study actually lacked JHs or JH signaling. These results demonstrate that the JH–Met–Kr-h1 signaling pathway (37–39) is functional during both the embryonic and early larval stages.

broad Is Essential for the Juvenile–Adult Transition in *Bombyx*. We further examined the roles of a pupal specifier gene, *broad*, in *Bombyx*, which is induced dramatically from the middle stage of the last instar (Fig. 6*A*) and signifies pupal commitment (1, 3, 20–22, 40). We injected TALEN mRNAs that targeted the core
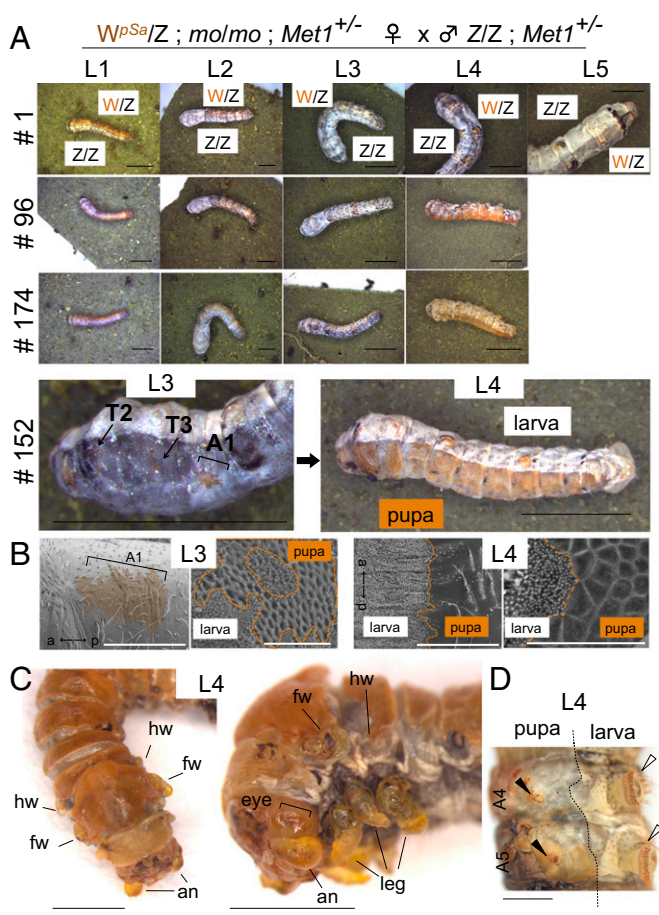
Fig. 5. Mosaic analysis of *Met1*. (*A*) Representative images of mosaic larvae. The larvae were reared individually and photographed at each larval instar. Individual numbers are shown on the left, and larval instars are shown at the top. *Met1* mosaics (#96, 174, and 152) did not exhibit pupal characters during L1 or L2, but small pupal patches were formed in L3 (see the magnified view of #152). Many of the L3 *Met1* mosaics molted to L4 and became severe larval–pupal mosaics. (Scale bars: 2 mm, L1 and L2 and 5 mm, L3–L5). (*B*) SEM analyses of the cuticles of *Met1* mosaic larvae. Pupal patches in the A1 of an L3 larva and the dorsal region of an L4 mosaic larva are shown. Magnified views are shown on the right. Note the presence of characteristic pupal cuticles. The anterior (a) and posterior (p) axes are indicated also. (Scale bars: 500 μm, *Left* and 50 μm, *Right*). (*C*) The most severe example of a *Met1* mosaic L4 larva. In this L4 larva, imaginal primordia grew considerably. Note the everted wing discs and the growth of imaginal compound eyes, antennae, and legs. an, antennae; eye, compound eyes; fw, forewings; hw, hindwings; leg, thoracic legs. (Scale bars: 2 mm.) (*D*) A mosaic larva whose abdominal prolegs were degenerated. Black and white arrowheads indicate degenerate and normal larval abdominal legs, respectively. (Scale bar: 1 mm.)

region of *broad* (22) into early embryos, and we investigated the phenotypes of the hatched larvae (Fig. 7 and Fig. S7). Among 192 injected eggs, 114 (59%) hatched, and 87 became pupae without apparent abnormalities during the larval stages. However, 53 of these 87 pupae had white patches on their pupal cuticles (Fig. 7*A*). SEM analysis showed that these white patches possessed the characteristic structures of larval cuticles, suggesting that the epidermal cells in the *broad* mutants were not pupally committed during L5, and these cells underwent larval–larval molt at the time of larval–pupal metamorphosis by the host. Surprisingly, 35 of the 53 larval–pupal mosaic pupae survived and emerged as larval–adult mosaic moths (Fig. 7*B*). Therefore, our mosaic analysis of *broad* suggests that the larval epidermal cells are not pupally committed in the absence of

broad, and thus they repeat larval–larval molts, although the hosts metamorphosed into pupae and adults. These results clearly indicate that *broad* is essential for the juvenile–adult transition in *Bombyx*, as found in other holometabolous insects (19, 21, 41–45).

Given the results of mosaic analysis, we further examined the expression of *broad* mRNAs in JH-deficient and JH signaling-deficient mutant *Bombyx* (Fig. 6 and Fig. S6). In *Manduca*, it has been shown that 20-hydroxyecdysone (20E) acting in the absence of JH is sufficient to induce *broad* expression at pupal commitment (19, 21, 45). Therefore, we consider that *broad* may be induced prematurely in JH-deficient or JH signaling-deficient mutant *Bombyx* larvae. However, the *broad* expression levels remained very low during the embryonic (Fig. S6) and early larval stages (Fig. 6), irrespective of the presence or absence of JHs or JH signaling. This result indicates that, in contrast to the proposed model of pupal commitment, which is based mainly on the data obtained from penultimate and last-instar larvae (19–21, 45), the absence of JHs is not sufficient to allow 20E-mediated induction of *broad*. Therefore, our results suggest that, in addition to the clearance of JHs from the body, another unidentified factor or signal is required for the 20E-induced expression of *broad*.

Discussion

The data presented here have two significant implications. First, we provide definitive evidence that JHs or the JH-signaling pathway is not necessary to maintain larval status during the early larval stages (Fig. S5), and this evidence suggests that successive larval instars are not iterations of the same program. Second, our results suggest that the inability of early-instar larvae to undergo metamorphosis, irrespective of the presence or absence of JHs, may be attributable to the regulatory mechanisms of *broad*, which is essential for pupal commitment.

A key finding of our study was that even in the absence of JHs or JH receptors, pupal characteristics were not observed in L1 or L2 in *Bombyx*. A small proportion of the epidermal cells were pupally committed during L2, but most other parts of the epidermis or imaginal primordia were not pupally committed until L3, and they metamorphosed at the molt from L3 to L4. This clear difference between L2 and L3 larvae may reflect a physiological difference between the two instars. In this study, we obtained definitive evidence supporting the hypothesis that there are two phases in the life of both holometabolous and hemimetabolous larvae (6–8): (*i*) a JH-independent phase (L1 and L2) in which JH does not have an important function and (*ii*) a JH-dependent phase (L3 and thereafter) in which the antimetamorphic action of JH is required to prolong the larval stage until the attainment of appropriate size for metamorphosis.

It has been shown that there are extensive differences in the roles of JHs during embryogenesis in holometabolous and hemimetabolous insects (27, 29, 46). Exogenous applications of JHs to the embryos of holometabolous insects elicit minor effects (27), whereas the application of JHs to the embryos of hemimetabolous (46) and ametabolous insects (47) has dramatic effects and disrupts normal embryogenesis. The knockout *Bombyx* lines generated in this study allowed us to test the effects of JH deprivation or JH signaling deprivation during the embryonic stages in lepidopteran insects. Our results provide genetic evidence that embryonic growth and morphogenesis in *Bombyx* are largely independent of JHs. Depriving *Bombyx* embryos of JHs or JH signaling decreased their hatchability and delayed hatching, but embryonic growth and morphogenesis were completed within their eggshells. The "unhatched" phenotype of JH-deficient mutants is unique because it can be rescued by dechorionation, and the rescued larvae are viable. Clearly, the hatching behaviors of lepidopteran embryos are under the control of circadian rhythms, and it has been suggested that they are
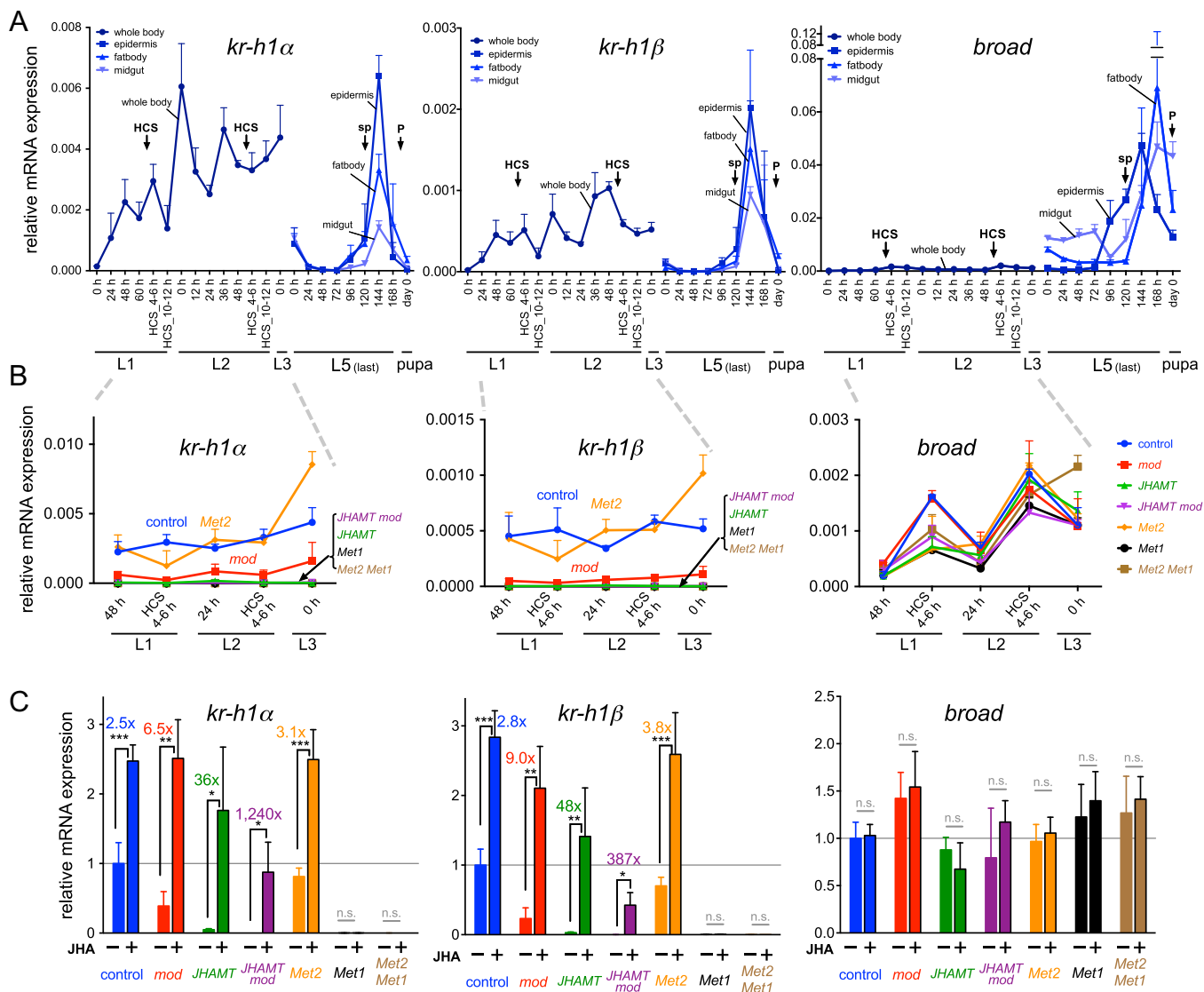
Fig. 6. qRT-PCR of *Kr-h1* and *broad*. (*A*) Expression levels of *Kr-h1α*, *Kr-h1β*, and *broad* mRNAs in the control strain during L1–L3 (whole body), L5, and pupa (epidermis, fat body, and midgut). The relative mRNA expression levels normalized against *rp49* are shown. The stages of the samples are shown below. Results represent mean + SD values (*n* = 4 biological replicates). HCS, head capsule slippage; P, pupation; sp, onset of spinning. (*B*) Expression levels of *Kr-h1α*, *Kr-h1β*, and *broad* mRNAs during the early larval instars of mutants. Total RNA was extracted from the whole body using individually genotyped samples (*Materials and Methods*). Relative mRNA expression levels normalized against *rp49* are shown. As shown in a previous study (6), the *Kr-h1* expression levels were lower in the *mod* strain than in the control. Note the very low levels of *Kr-h1* mRNA in *JHAMT*, *JHAMT mod*, *Met1*, and *Met2 Met1* mutants. In the mutants used in this study, *broad* expression was comparable with that in the control, but it remained at a very low level. Note that the *y*-axis scales differ in *A* and *B*. The data represent the mean + SD (*n* = 3–5 biological replicates). (*C*) Effects of methoprene treatment on gene expression levels. L1 larvae (24 h after hatching) were treated topically with 0.1 μg of methoprene (+) or solvent alone (acetone) (−), and total RNA was extracted from the whole body of each individual 24 h after the treatment. Values represent the mean + SD (*n* = 3–5) normalized against the value of the control strain treated with acetone (set to 1). The values of fold changes are indicated above the bars. Asterisks indicate significant differences compared with the control values according to the Student's *t* test: *$P < 0.05$; **$P < 0.01$; ***$P < 0.001$. n.s., not significant.

controlled by brain-derived factors (30, 31). However, these factors or hormones have not yet been identified. We suggest that JHs may be involved in some aspects of embryonic neurogenesis, and thus the loss of JHs affects hatching behavior. It should be noted that almost all the mutant lines used in this study had a *white-1* (*w-1*) mutant background, which lacked the ommochrome pigments in the eyes and eggs (48). The *w-1* mutant background may have affected the hatchability of the mutants, because *Drosophila cinnabar* (*cn*) mutants, a counterpart of *Bombyx w-1*, and *Drosophila white* mutants exhibit some neural defects (49). Truman and Riddiford (29) have proposed that the ancestral role of JH was controlling aspects of embryogenesis and that a

shift in the timing of JH secretion during embryonic and post-embryonic development may have led to evolutionary changes from ametabolous to hemimetabolous and holometabolous insects. Thus it is of interest to compare the effects of JH deprivation and JH signaling deprivation on embryogenesis in diverse insect groups, including ametabolous and hemimetabolous insects.

During the diversification of various insect groups, *Met* genes have been duplicated independently at least two times, because two paralogs are present in *Drosophila* (*Met* and *gce*) and *Bombyx* (*Met1* and *Met2*) (23–25). In *Drosophila*, single mutants of *Met* or *gce* are viable and fertile, but their double mutants die during the late prepupal stages without reducing the number of larval molts
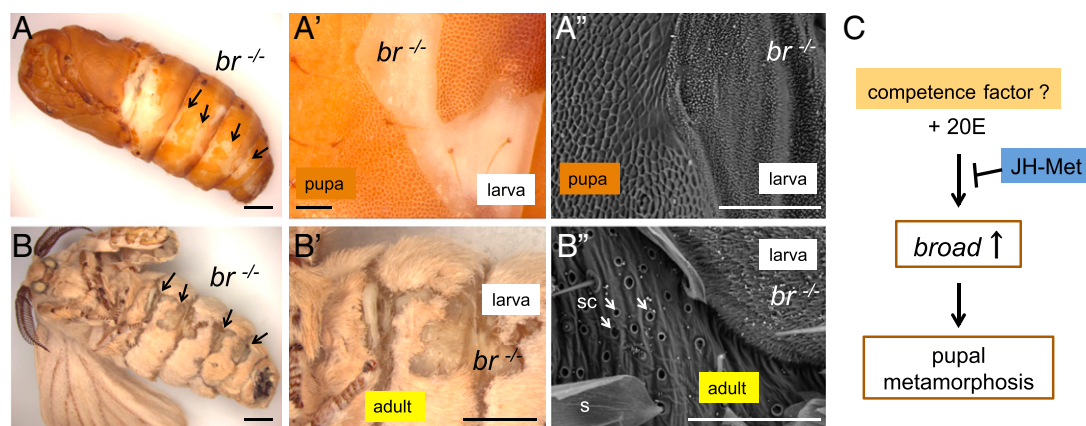
Fig. 7. *broad* is essential for pupal metamorphosis in the epidermis. (*A*) Representative image of a mosaic pupa with patches of larval cuticles. TALEN mRNAs that targeted *broad* were injected into embryos, and the hatched larvae were subjected to the phenotypic analysis. (*B*) The animal shown in *A*. This pupa metamorphosed into a moth with larval–adult mosaic cuticles. Arrows in *A* and *B* indicate the positions of larval patches. Magnified views of mosaic cuticles are shown in *A'* and *B'*. SEM analyses showed that the "white" cuticles actually exhibited the characteristic structures of larval cuticles (*A''* and *B''*). s, scale; sc, socket cells (indicated by white arrows). (Scale bars: 2 mm in *A*, *B*, and *B'*, 0.2 mm in *A'*, and 0.1 mm in *A''* and *B''*). (*C*) Hypothetical model of the regulatory mechanism of *broad*. We assume that the presence of a *broad*-inducing factor, or competence factor, is required for the up-regulation of *broad* that leads to pupal commitment (*Discussion*). Tissues in L1 larvae and most tissues in L2 larvae are not pupally committed, irrespective of the presence or absence of JH, because of the absence or very low levels of this competence factor. After L3, larvae can be pupally committed because of the presence or high levels of this factor, but its action is repressed by JHs, as demonstrated in the later stages in *Manduca* and *Bombyx* (19–21, 45). In the last instar, the JH titer decreases to a very low level, and thus *broad* can be strongly induced by the putative factor and 20E, thereby leading to pupal metamorphosis.

(23, 24). This observation suggests that the functions of the two JH receptors largely overlap in *Drosophila*. In contrast, our results demonstrated the nonoverlapping functions of the two receptors in *Bombyx*. We observed no specific phenotypes in *Met2* mutants with respect to their morphology, viability, fertility, or *Kr-h1* mRNA expression levels. Importantly, the *Met2 Met1* double mutants almost completely phenocopied *Met1* mutants, and the JH-mediated induction of *Kr-h1* was totally dependent on the presence of a functional *Met1* during the embryonic and larval stages. This finding demonstrates that *Met1* is the predominant JH receptor, at least during the embryonic and larval stages. Previously, based on in vitro experiments (15), we proposed that Met2 forms a complex with its partner Taiman/SRC and binds to a JH-responsible element of *Kr-h1*, thereby activating its transcription in a JH-dependent manner, but the in vivo role of Met2 is still unclear. The *Met2* mRNA expression levels are very low compared with those of *Met1* throughout embryonic and larval development, but they increase greatly from the late pupal stage and are maintained at very high levels during the adult stages (50). Therefore, it is possible that the two receptors control different developmental programs in lepidopteran insects, so that *Met1* is required for the antimetamorphic actions of JHs, and *Met2* is required for the JH-mediated reproductive maturation of adults. We anticipate that the role of *Met2* may be demonstrated clearly in studies using other lepidopteran species because, unlike many moth species, newly emerged *Bombyx* adults are reproductively mature, even though their CA is removed during the larval stages.

The results of the present study also are important in methodological terms. We used two approaches for mosaic analyses. In the mosaic analysis of *Met1*, we first established a mutant line, and then the mutant allele was introduced into a hereditary mosaic strain by crossing. In the mosaic analysis of *broad*, we injected TALEN mRNAs into embryos, and the hatched larvae were subjected to direct phenotypic analysis. Given that a number of genes have been targeted in *Bombyx* since the recent development of genome-editing tools (16, 17), the former approach is very useful and could become a standard technique for functional studies of *Bombyx* genes. The latter approach facili-

tates the more rapid characterization of genes and in principle can be applied to a wide variety of animals. In particular, we found that the severity of the mosaic phenotypes could be controlled to some extent by changing the injected doses of TALEN mRNAs (*Materials and Methods*). Therefore, mosaic analysis using the latter approach will facilitate functional studies of genes in nonmodel insects and other arthropods, because RNAi has been almost the only method used for the in vivo characterization of target genes in these species.

We showed that *broad* is essential for pupal commitment and morphogenesis, at least in the epidermis of *Bombyx*. Previous RNAi analyses of *Bombyx broad* using a recombinant Sindbis virus vector showed that the loss of *broad* function disrupted the formation of adult eyes, legs, and wings, and programmed cell death was induced in the larval silk glands (40). However, because this virus did not appear to infect the epidermal cells, it was not clear whether pupal metamorphosis in the epidermis is also dependent on *broad* (40). Our results clearly demonstrate that *broad* is essential for pupal commitment in the epidermis. Surprisingly, epidermal cells without a functional *broad* gene exhibited repeated larval–larval molts at the time of host metamorphosis to produce larval–pupal and larval–adult mosaics. It is not clear why *broad*-mutant larval epidermal cells did not produce adult cuticles directly (i.e., direct metamorphosis from larva to adult) at the time of pupal–adult metamorphosis by hosts. One explanation is that the *Bombyx* epidermis will not commit to becoming an adult unless it already has been pupally committed. Recently, it was shown that an ecdysone-inducible gene, *E93*, acts as an adult specifier in both holometabolous and hemimetabolous insects (39, 51). Therefore, future studies should investigate the regulatory mechanisms of the adult specifier *E93* and the genetic interactions between *broad* and *E93*. It also is noteworthy that, in imaginal tissues, direct metamorphosis from larva to adult can be induced in some insect species. For example, in the cecropia moth (*Hyalophora cecropia*) and in the red flour beetle (*Tribolium castaneum*), last-instar larvae that receive allatectomy or RNAi of *Met* transform into pupae with extensive adult characters such as compound eyes, antennae, and wings (52, 53). However, the allatectomized or knockout *Bombyx* larvae

used in this study did not exhibit such an adult overshoot. It has been proposed that this difference is caused by the different timing of the decisions for pupal versus adult fates in imaginal tissues, i.e., before or after the prepupal ecdysteroid peak (54).

A final question raised by our results is what factors or signals confer competence for pupal metamorphosis in larvae, because the absence of JHs or JH signaling alone did not render insect larvae competent for metamorphosis. In contrast to the previously proposed model, in which JH inhibits the 20E-mediated up-regulation of *broad* (19–21, 45), we showed that the loss of JH is not sufficient to induce *broad* during L1 or L2 in *Bombyx*. Thus, given that *broad* is essential for pupal commitment in the epidermis of *Bombyx* and that *broad* overexpression is sufficient to induce precocious metamorphosis in *Drosophila* (19, 44), we suggest that the lack of competence in early-instar larvae may be attributable to the absence of factors or signals required to induce *broad*. According to the classic experiments by Piepho (55, 56), the epidermis of L1 larvae of the greater wax moth *Galleria mellonella* can pupate directly when implanted into the last-instar larvae. This finding suggests that L1 epidermis can be pupally committed if some blood-borne factors are provided by the hosts during the last instar. Therefore, we consider that the *broad*-inducing factor, or competence factor, may be a humoral factor. The absence or very low levels of this competence factor may explain why L1 larvae and most tissues of L2 larvae are incompetent to metamorphose (Fig. 7C).

It has been suggested that JHs and their homologs (e.g., MF in crustaceans) originated more than 500 million years ago (57) at an early stage of arthropod evolution and that their ancestral roles were in reproduction (58). Subsequently, the roles of JHs diversified extensively in insect lineages, and JHs now play key roles in regulating development, metamorphosis, reproduction, diapause, behavior, and polyphenism in insects (59, 60). Recent rapid advances in genome-editing tools facilitate the efficient editing of genes or genomes in both model and nonmodel organisms (61–63). Thus, we are hopeful that the present study will encourage further research into the molecular mechanisms of JH actions in diverse insect groups and other arthropods, thereby yielding a better understanding of how JHs have acquired antimetamorphic actions as well as other pleiotropic actions during the evolution of insects.

Materials and Methods

Strains. Silkworms were reared on an artificial diet at 25–27 °C under standard conditions as described previously (64). Knockout *Bombyx* were generated using TALENs, as described previously (16, 17). Briefly, TALEN mRNAs (400 ng/μL) were injected into *pnd w-1* embryos (65). Established knockout lines of *JHAMT*, *Met2*, *Met1*, and *Met2 Met1* were not outcrossed to other standard strains so that we could compare the phenotypes and gene-expression levels in the same genetic background (i.e., *pnd w-1*). *JHAMT mod* double mutants were established after crossing *JHAMT*+/− adults with the *w-1 mod* strain (6, 7) in the *w-1 pnd*+ background. Eggs of *JHAMT mod* double mutants and *Met1* mosaic strain were treated with HCl at ~20 h AO to cancel the diapause of eggs (66); eggs in other strains were not treated. Mutant lines with *JHAMT*- or *Met1*-mutant alleles were maintained as heterozygous stocks: adults were genotyped at each generation to obtain egg batches from sibling crosses of heterozygous adults. The parental *pnd w-1* strain was used as a control strain throughout this study. Note that *Met2* gene is located on the Z chromosome. In some cases, we abbreviate *Met2* homozygous or hemizygous mutants as *Met2*−/−, but this abbreviation does not indicate that they are males. The nucleotide sequences of the generated knockout alleles and TALEN target sites are shown in Fig. S1.

Genotyping and Phenotypic Analysis. For genotyping, samples were crushed in alkaline buffer (50 mM NaOH, 0.2 mM EDTA) and then heated at 95 °C for 10–15 min. After neutralization with the same volume of 0.2 M Tris·HCl (pH 8.0), the supernatants were used as templates for PCR. If genotyping of RNA samples was necessary, samples from individual animals were homogenized in Buffer RLT Plus (Qiagen) or TRIzol (Invitrogen). Next, 10-μL aliquots were used for genomic DNA (gDNA) extraction. To precipitate gDNAs from the aliquots, a 0.3× volume of 3 M sodium acetate (pH 5.2) and a 10× volume of ethanol were added and vortexed. After centrifugation at 20,000 × g for 20 min at 4 °C, the pellets were rinsed once with 70% (vol/vol) ethanol, dissolved in 20 μL of distilled water, and used as templates for PCR. The primers used in this study are listed in Table S1. All (for control and mutants of *mod* and *Met2*) or about one-fourth (for the other mutant strains) of the eggs from each batch (n = 4–15 batches for each genotype) were used to determine the hatchability and day of hatching. Hatched larvae were collected daily in individual 96-well plates, and unhatched eggs were collected on day 17 AO (most of the larvae hatched on day 10). Because we often failed to genotype embryos before stage 25 (pigmentation of trachea; day 7 after AO) (66), which comprised less than 10% of the total eggs, we examined unhatched embryos only at stage 25 or later. We diluted JH III (Sigma-Aldrich), methoprene (a kind gift from S. Sakurai, Kanazawa University, Japan), and MF (SDS Biotech) with acetone and then applied selected doses. In the dechorionation experiments, the chorions of eggs were removed with a sharp knife on day 12 AO. SEM analyses were performed using a low-vacuum scanning electron microscopye (MiniScope TM1000; Hitachi High Technologies). Specimens were fixed in 70% (vol/vol) ethanol and stored at 4 °C. The specimens were air dried for several minutes and mounted directly on the stage without further treatment.

Quantitative RT-PCR and Whole-Mount in Situ Hybridization. Total RNA was extracted using an RNeasy Plus mini kit (Qiagen) or TRIzol reagent and was used to synthesize cDNA with a PrimeScript RT reagent kit (TaKaRa) or ReverTra Ace qPCR RT Master Mix with a gDNA Remover kit (ToYoBo). Quantitative PCR (qPCR) was performed as described previously (15). The expression levels of the target genes were normalized against that of *rp49*. Whole-mount in situ hybridization in embryos was performed as described previously (68).

Mosaic Analysis of *Met1* and *broad*. To establish a mosaic strain of *Met1*, *Met1* heterozygote males were crossed with females of a hereditary mosaic strain, m042 (Kyushu University) (69). After several generations, the *Met1* mosaic strain was genetically fixed and maintained by the following cross: T(W;2)p^{Sa}/Z; *mo/mo*; *Met1*+/−; *w-2*+/− ♀ × ♂ Z/Z; *mo/mo* or *mo/+*; *Met1*+/−; *w-2*−/−. In this strain, the fertilization of polar body nuclei, which yields mosaic animals, could be detected by the mosaic pigmentation patterns on the amnioserosa of eggs (mosaics of *w-2*+/− and *w-2*−/−, which were black and white, respectively) and pigmentation of the larval cuticles [mosaics of T(W;2)p^{Sa}/Z and Z/Z with pigmented and nonpigmented larval cuticles, respectively; see individual #1 in Fig. 5A]. In the mosaic analysis of *Met1*, eggs with mosaic color patterns were collected, and the hatched larvae were individually reared. When a standard dose (400 ng/μL) (16, 17) of TALEN mRNAs that targeted the core region of *broad* was injected into embryos, all the hatched larvae died by the pharate pupal stages. Because this phenotype appeared to be too strong for mosaic analysis, we greatly reduced the dose of injected TALEN mRNAs. When 100-fold lower doses (4 ng/μL) were injected, many larvae survived until they became pupae and adults, thereby allowing observation of the mosaic phenotypes in the pupal and adult stages. A summary of the mosaic analysis of *broad* is shown in Fig. S7.

1. Jindra M, Palli SR, Riddiford LM (2013) The juvenile hormone signaling pathway in insect development. *Annu Rev Entomol* 58:181–204.
2. Riddiford LM (1996) Juvenile hormone: The status of its "status quo" action. *Arch Insect Biochem Physiol* 32(3-4):271–286.
3. Riddiford LM (2012) How does juvenile hormone control insect metamorphosis and reproduction? *Gen Comp Endocrinol* 179(3):477–484.
4. Niwa R, Niwa YS (2014) Enzymes for ecdysteroid biosynthesis: Their biological functions in insects and beyond. *Biosci Biotechnol Biochem* 78(8):1283–1292.
5. Daimon T, Shinoda T (2013) Function, diversity, and application of insect juvenile hormone epoxidases (CYP15). *Biotechnol Appl Biochem* 60(1):82–91.
6. Smykal V, et al. (2014) Importance of juvenile hormone signaling arises with competence of insect larvae to metamorphose. *Dev Biol* 390(2):221–230.

7. Daimon T, et al. (2012) Precocious metamorphosis in the juvenile hormone-deficient mutant of the silkworm, *Bombyx mori*. *PLoS Genet* 8(3):e1002486.

8. Tan A, Tanaka H, Tamura T, Shiotsuki T (2005) Precocious metamorphosis in transgenic silkworms overexpressing juvenile hormone esterase. *Proc Natl Acad Sci USA* 102(33):11751–11756.

9. Abdou MA, et al. (2011) *Drosophila* Met and Gce are partially redundant in transducing juvenile hormone action. *Insect Biochem Mol Biol* 41(12):938–945.

10. Riddiford LM, Truman JW, Mirth CK, Shen YC (2010) A role for juvenile hormone in the prepupal development of *Drosophila melanogaster*. *Development* 137(7):1117–1126.

11. Bounhiol J (1938) Recherches experimentales sur le determinisme de la metamorphose chez les Lepidopteres. *Bull Biol Fr Belg* 24:1–199.

12. Fukuda S (1944) The hormonal mechanism of larval molting and metamorphosis in the silkworm. *J Fac Sci Tokyo Univ Sect IV* 6:477–532.

13. Aboulafia-Baginsky N, Pener MP, Staal GB (1984) Chemical allatectomy of late *Locusta* embryos by a synthetic precocene and its effect on hopper morphogenesis. *J Insect Physiol* 30(11):839–852.

14. Furuta K, et al. (2007) Synthesis and anti-juvenile hormone activity of ethyl 4-(2-benzylalkyloxy)benzoates and their enantiomers. *J Pestic Sci* 32(2):99–105.

15. Kayukawa T, et al. (2012) Transcriptional regulation of juvenile hormone-mediated induction of *Krüppel homolog 1*, a repressor of insect metamorphosis. *Proc Natl Acad Sci USA* 109(29):11729–11734.

16. Daimon T, Kiuchi T, Takasu Y (2014) Recent progress in genome engineering techniques in the silkworm, *Bombyx mori*. *Dev Growth Differ* 56(1):14–25.

17. Takasu Y, et al. (2013) Efficient TALEN construction for Bombyx mori gene targeting. *PLoS One* 8(9):e73458.

18. Shinoda T, Itoyama K (2003) Juvenile hormone acid methyltransferase: A key regulatory enzyme for insect metamorphosis. *Proc Natl Acad Sci USA* 100(21):11986–11991.

19. Zhou X, Riddiford LM (2002) Broad specifies pupal development and mediates the 'status quo' action of juvenile hormone on the pupal-adult transformation in *Drosophila* and *Manduca*. *Development* 129(9):2259–2269.

20. Muramatsu D, Kinjoh T, Shinoda T, Hiruma K (2008) The role of 20-hydroxyecdysone and juvenile hormone in pupal commitment of the epidermis of the silkworm, *Bombyx mori*. *Mech Dev* 125(5-6):411–420.

21. Zhou B, Hiruma K, Shinoda T, Riddiford LM (1998) Juvenile hormone prevents ecdysteroid-induced expression of *broad complex* RNAs in the epidermis of the tobacco hornworm, *Manduca sexta*. *Dev Biol* 203(2):233–244.

22. Reza AM, et al. (2004) Hormonal control of a metamorphosis-specific transcriptional factor Broad-Complex in silkworm. *Comp Biochem Physiol B Biochem Mol Biol* 139(4):753–761.

23. Baumann AA, Wilson TG (2011) Molecular evolution of juvenile hormone signaling. *Gene Duplication*, ed Friedberg F (InTech, Rijeka, Croatia), pp 332–352.

24. Baumann A, Fujiwara Y, Wilson TG (2010) Evolutionary divergence of the paralogs *Methoprene tolerant* (*Met*) and *germ cell expressed* (*gce*) within the genus *Drosophila*. *J Insect Physiol* 56(10):1445–1455.

25. Jindra M, et al. (2015) Genetic evidence for function of the bHLH-PAS Protein Gce/Met as a Juvenile Hormone receptor. *PLoS Genet* 11(7):e1005394.

26. Oota S, Watanabe A, Tokunaga H (1956) Genetical study on a spontaneous mutant, two molter, in the silkworm, *Bombyx mori*. *J Insect Biotec Seric* 26(1):77–81.

27. Riddiford LM, Williams CM (1967) The effects of juvenile hormone analogues on the embryonic development of silkworms. *Proc Natl Acad Sci USA* 57(3):595–601.

28. Bergot BJ, Baker FC, Cerf DC, Jamieson G, Schooley DA (1981) Qualitative and quantitative aspects of juvenile hormone titers in developing embryos of several insect species: Discovery of a new JH-like substance extracted from eggs of Manduca sexta. *Juvenile Hormone Biochemistry*, eds Pratt GE, Brooks GT (Elsevier, Amsterdam), pp 33–45.

29. Truman JW, Riddiford LM (1999) The origins of insect metamorphosis. *Nature* 401(6752):447–452.

30. Sauman I, Reppert SM (1998) Brain control of embryonic circadian rhythms in the silkmoth Antheraea pernyi. *Neuron* 20(4):741–748.

31. Sauman I, Tsai T, Roca AL, Reppert SM (1996) Period protein is necessary for circadian control of egg hatching behavior in the silkmoth *Antheraea pernyi*. *Neuron* 17(5):901–909.

32. Yamaguchi J, et al. (2013) Periodic *Wnt1* expression in response to ecdysteroid generates twin-spot markings on caterpillars. *Nat Commun* 4:1857.

33. Kobayashi M (1991) Mutation of meiotic division and fertilization. *Iden* 45:14–18. Japanese.

34. Fujii T, Abe H, Yamamoto K, Katsuma S, Shimada T (2011) Interspecies linkage analysis of *mo*, a *Bombyx mori* locus associated with mosaicism and gynandromorphism. *Genetica* 139(10):1323–1329.

35. Goldschmidt R, Katsuki K (1931) Vierte mitteilung uber erblichen gynandromorphismus und somatische mosaikbildung bei *Bombyx mori* L. *Biol Zent Bl* 51:58–74.

36. Fristrom D, Fristrom JW (1993) The metamorphic development of the adult epidermis. *The Development of Drosophila melanogaster*, eds Bate M, Arias AM (Cold Spring Harbor Lab Press, Plainview, NY), pp 843–897.

37. Konopova B, Jindra M (2007) Juvenile hormone resistance gene *Methoprene-tolerant* controls entry into metamorphosis in the beetle *Tribolium castaneum*. *Proc Natl Acad Sci USA* 104(25):10488–10493.

38. Minakuchi C, Namiki T, Shinoda T (2009) *Krüppel homolog 1*, an early juvenile hormone-response gene downstream of *Methoprene-tolerant*, mediates its anti-metamorphic action in the red flour beetle *Tribolium castaneum*. *Dev Biol* 325(2):341–350.

39. Belles X, Santos CG (2014) The MEKRE93 (Methoprene tolerant-Krüppel homolog 1-E93) pathway in the regulation of insect metamorphosis, and the homology of the pupal stage. *Insect Biochem Mol Biol* 52:60–68.

40. Uhlirova M, et al. (2003) Use of Sindbis virus-mediated RNA interference to demonstrate a conserved role of Broad-Complex in insect metamorphosis. *Proc Natl Acad Sci USA* 100(26):15607–15612.

41. Konopova B, Jindra M (2008) Broad-Complex acts downstream of Met in juvenile hormone signaling to coordinate primitive holometabolan metamorphosis. *Development* 135(3):559–568.

42. Parthasarathy R, Tan A, Bai H, Palli SR (2008) Transcription factor broad suppresses precocious development of adult structures during larval-pupal metamorphosis in the red flour beetle, *Tribolium castaneum*. *Mech Dev* 125(3-4):299–313.

43. Suzuki Y, Truman JW, Riddiford LM (2008) The role of Broad in the development of *Tribolium castaneum*: Implications for the evolution of the holometabolous insect pupa. *Development* 135(3):569–577.

44. Zhou X, Zhou B, Truman JW, Riddiford LM (2004) Overexpression of *broad*: A new insight into its role in the *Drosophila* prothoracic gland cells. *J Exp Biol* 207(Pt 7):1151–1161.

45. Zhou B, Riddiford LM (2001) Hormonal regulation and patterning of the broad-complex in the epidermis and wing discs of the tobacco hornworm, *Manduca sexta*. *Dev Biol* 231(1):125–137.

46. Erezyilmaz DF, Riddiford LM, Truman JW (2004) Juvenile hormone acts at embryonic molts and induces the nymphal cuticle in the direct-developing cricket. *Dev Genes Evol* 214(7):313–323.

47. Rohdendorf EB, Sehnal F (1973) Inhibition of reproduction and embryogenesis in the fireblat, *Thermobia domestica*, by juvenile hormone analogues. *J Insect Physiol* 19(1):37–56.

48. Quan GX, et al. (2002) Characterization of the *kynurenine 3-monooxygenase* gene corresponding to the *white egg 1* mutant in the silkworm *Bombyx mori*. *Mol Genet Genomics* 267(1):1–9.

49. McRobert SP, et al. (2003) Mutations in raised *Drosophila melanogaster* affect experience-dependent aspects of sexual behavior in both sexes. *Behav Genet* 33(3):347–356.

50. Kayukawa T, Shinoda T (May 7, 2015) Functional characterization of two paralogous JH receptors, methoprene-tolerant 1 and 2, in the silkworm, *Bombyx mori* (Lepidoptera: Bombycidae). *Appl Entomol Zool*, 10.1007/s13355-015-0345-8.

51. Ureña E, Manjón C, Franch-Marro X, Martín D (2014) Transcription factor E93 specifies adult metamorphosis in hemimetabolous and holometabolous insects. *Proc Natl Acad Sci USA* 111(19):7024–7029.

52. Williams CM (1961) The juvenile hormone. II. Its role in the endocrine control of molting, pupation, and adult development in the cecropia silkworm. *Biol Bull* 121(3):572–585.

53. Parthasarathy R, Tan A, Palli SR (2008) bHLH-PAS family transcription factor methoprene-tolerant plays a key role in JH action in preventing the premature development of adult structures during larval-pupal metamorphosis. *Mech Dev* 125(7):601–616.

54. Truman JW, Riddiford LM (2002) Endocrine insights into the evolution of metamorphosis in insects. *Annu Rev Entomol* 47:467–500.

55. Piepho H (1938) Wachstum und totale Metamorphose an Hautimplantaten bei der Wachsmotte Galleria mellonella L. *Biol Zbl* 58:356–366.

56. Piepho H (1938) Uber die Auslosung der Raupenhautung,Verpuppung und Imaginalentwicklung an Hautimplantaten von Schmetterlingen. *Biol Zbl* 58:481–495.

57. Sehnal F (1984) The juvenile hormone of insects. *Nova Acta Leopold* 56:251–266.

58. Wyatt GR (1997) Juvenile hormone in insect reproduction–a paradox? *Eur J Entomol* 94:323–333.

59. Goodman WG, Cusson M (2012) The juvenile hormones. *Insect Endocrinology*, ed Gilbert LI (Elsevier, London), pp 311–365.

60. Nijhout HF (1998) *Insect Hormones* (Princeton Univ Press, Princeton, NJ).

61. Joung JK, Sander JD (2013) TALENs: A widely applicable technology for targeted genome editing. *Nat Rev Mol Cell Biol* 14(1):49–55.

62. Hwang WY, et al. (2013) Efficient genome editing in zebrafish using a CRISPR-Cas system. *Nat Biotechnol* 31(3):227–229.

63. Nakade S, et al. (2014) Microhomology-mediated end-joining-dependent integration of donor DNA in cells and animals using TALENs and CRISPR/Cas9. *Nat Commun* 5:5560.

64. Daimon T, et al. (2003) A *Bombyx mori* gene, BmChi-h, encodes a protein homologous to bacterial and baculovirus chitinases. *Insect Biochem Mol Biol* 33(8):749–759.

65. Tamura T, et al. (2000) Germline transformation of the silkworm *Bombyx mori* L. using a *piggyBac* transposon-derived vector. *Nat Biotechnol* 18(1):81–84.

66. Tazima Y (1978) *The Silkworm: An Important Tool* (Kodansha, Tokyo).

67. Takami T, Kitazawa T (1960) External observation of embryonic development in the silkworm. *Bull Seric Exp Sta (Tokyo)* 75:1–31.

68. Nakao H, Matsumoto T, Oba Y, Niimi T, Yaginuma T (2008) Germ cell specification and early embryonic patterning in *Bombyx mori* as revealed by *nanos* orthologues. *Evol Dev* 10(5):546–554.

69. Banno Y, et al. (2005) *A Guide to the Silkworm Mutants 2005-Gene name and Gene* (Silkworm Genetics Division, Institute of Genetic Resorces, Kyushu University, Fukuoka, Japan).

70. Kayukawa T, et al. (2014) Hormonal regulation and developmental role of Krüppel homolog 1, a repressor of metamorphosis, in the silkworm *Bombyx mori*. *Dev Biol* 388(1):48–56.